Inhibition of galectin-1 ligand synthesis accentuates anti-tumor immunity.

Filiberto Cedeno-Laurent[1,3,7], Matthew Opperman[1,7], Steven R. Barthel[1,3], Danielle Hays[1], Tobias Schatton[1,4], Qian Zhan[2], Xiaoying He[3,5], Khushi L. Matta[6], Jeffrey G. Supko[3,5], Markus H. Frank[1,4], George F. Murphy[2,3], and Charles J. Dimitroff[1,3,8]

[1]Department of Dermatology
[2]Department of Pathology
Brigham and Women's Hospital
Boston, MA 02115

[3]Harvard Medical School
Boston, MA 02115

[4]Transplantation Research Center
Children's Hospital
Boston, MA 02115

[5]Massachusetts General Hospital
Department of Medicine
55 Fruit Street
Boston, MA, 02114

[6]Roswell Park Cancer Institute
Department of Cancer Biology
Elm and Carlton Sts.
Buffalo, NY 14263

[7]These authors contributed equally to this work.

[8]To whom correspondence should be addressed:
Charles J. Dimitroff, Ph.D.
HIM, Rm. 662
77 Avenue Louis Pasteur
Boston. MA 02115
Phone: 617-525-5693
Fax: 617-525-5571
E-mail: cdimitroff@rics.bwh.harvard.edu

Running Title: Gal-1 ligand suppression boosts anti-tumor immunity.

Abstract

Galectin-1 (Gal-1) has been shown to play a major role in tumor immune evasion by inducing apoptosis in Gal-1 ligand$^+$ effector T cells and by promoting the synthesis of T cell immunoregulatory molecules. However, little is known about Gal-1's spatial arrangement in tumor tissue with respect to tumor-infiltrating T cells and tumor-initiating cells. Here, we show that Gal-1 is often expressed in primary human melanomas as curvilinear arrays that strategically surround nests of ABCB5$^+$ melanoma-initiating cells, reminiscent of an immune-privileged site. To test the Gal-1-mediated immune evasion hypothesis and demonstrate the importance of Gal-1 ligands in controlling the fate and function of anti-tumor immune cells, we treated mice bearing syngeneic tumors with peracetylated 4-fluoro-glucosamine (4-F-GlcNAc), an inhibitor of Gal-1 ligand biosynthesis, and analyzed tumor growth and immune profiles. We found that 4-F-GlcNAc spared Gal-1-mediated apoptosis of anti-tumor cytotoxic and helper T cells and of NK cells by diminishing Gal-1 ligand expression. 4-F-GlcNAc-dependent T cell skewing caused elevations in tumor-specific cytotoxic T cells and IFN-γ, and reductions in T cell-associated immunoregulatory molecules, which collectively resulted in minimal tumor growth. These data implicate Gal-1 in the immunoprotection of tumor-initiating cells and show that inhibiting Gal-1 ligand synthesis can boost anti-tumor immunity.

Introduction

Galectin-1 (Gal-1), a soluble ß-galactoside-binding lectin, is becoming increasingly appreciated as a biological modifier of tumor growth and metastasis (1-6). Gal-1 can mediate autocrine and paracrine activities that favor invasiveness (7-13), drive angiogenesis (14, 15) and regulate anti-tumor immune responses (16-20). Gal-1 regulates the fate and function of effector leukocytes by inducing pro-apoptotic signals on effector leukocytes with concomitant skewing of cancer microenvironments towards Th2 and regulatory cytokine profiles (16-18, 20, 21).

Considering recent studies targeting Gal-1 for anti-cancer therapeutic exploitation (16-18, 21), few have focused on perturbing complementary Gal-1 ligands to counteract Gal-1-mediated tumor immune evasion. Gal-1 ligands are membrane proteins consisting of one or more N-acetyllactosamine Type1 (Galβ1,3GlcNAc) or Type 2 (Galβ1,4GlcNAc) disaccharides on N-linked and O-linked glycans (22, 23). Gal-1 ligands are expressed at a high level on activated CTLs and on pro-inflammatory Th1 and Th17 cell subsets, and, upon Gal-1-binding, transmit pro-apoptotic signals or promote regulatory cytokine production (24-26). Ligands identified to date include CD4, CD7, CD43 and CD45 among others (27). Thus, as effector T cells express robust levels of Gal-1 ligands, their viability is inherently limited in a tumor microenvironment rich in Gal-1. In fact, when tumor-derived Gal-1 is abrogated, enhanced levels IFN-γ-producing cells help prevent tumor progression (16, 18), or when Gal-1 ligand, CD43, is absent, tumor growth is impaired (15, 28).

Here, we show that Gal-1 in human melanomas is frequently arranged in a curvilinear pattern surrounding cells expressing the prospective marker of melanoma-initiating cells, ABCB5 (29, 30). Within these microenvironmental nests, tumor-infiltrating T cells were often excluded, preventing intimate contact with $ABCB5^+$ melanoma-initiating cells. To evaluate whether modifying Gal-1 ligands would impact anti-tumor immune responses, we treated mice bearing syngeneic B16 melanomas or EL-4 lymphomas with 4-F-GlcNAc, a biosynthetic inhibitor of Gal-1-binding N-acetyllactosamine moieties (8, 9, 31-33). 4-F-GlcNAc treatment inhibited Gal-1 ligand formation on effector T and NK cells, which prevented Gal-1-induced apoptosis and caused concomitant increases in melanoma-specific CTLs and IFN-γ levels. This immune profile corresponded with significant reductions in tumor

growth. These attenuated tumors were similar in size to those in mice deficient in Gal-1 or in mice deficient in Gal-1 ligand CD43 (24), demonstrating that host-derived Gal-1 and putative Gal-1 ligand, CD43, are important regulators of anti-tumor T cell immunity. These data suggest that Gal-1 is strategically oriented in human melanomas to provide immune protection from effector T cells and that interference of Gal-1 ligand synthesis on effector anti-tumor T cells represents a promising therapeutic approach to boost anti-tumor immune responses.

Materials and Methods

Mice, Cell Lines, Antibodies and Chemicals.

C57BL/6 wild type (wt) mice and Gal-1$^{-/-}$ mice were obtained from Jackson Laboratory. C57BL/6 CD43$^{-/-}$ mice were kindly provided by Dr. Hermann J. Ziltener (University of British Columbia, Canada). Immunodeficient mice lacking B, T and NK cells that deficient in *Rag2* and *Jak3* genes (Rag2$^{-/-}$/Jak3$^{-/-}$) were generated as described (34). Mouse J558L plasmacytoma cells, EL-4 lymphoma cells and B16F10 melanoma cells were purchased from American Type Culture Collection (ATCC™), Inc. ATCC routinely uses various molecular authentication tests to support their ATCC collections. These tests are supported by the ATCC Molecular Authentication Resource Center that includes the genomic core and by the immunology and proteomic cores. Antibodies included: anti-mouse/human Gal-1 (N16) and anti-mouse β-actin (Santa Cruz Biotechnology); alkaline phosphatase (AP)-conjugated anti-goat IgG (Southern biotech); allophycocyanin (APC)-conjugated anti-human Fc (Jackson Immunoresearch); anti-human Gal-1 (Sigma-Aldrich); FITC-labeled anti-mouse CD4, PE-labeled anti-mouse CD3, FITC-Annexin-V, APC-Cy7-anti-mouse CD19, PerCP Cy5.5 anti-mouse CD8, APC-conjugated anti-mouse CD25, FITC-anti mouse CD69, PerCP Cy5.5 anti-NK1.1, anti-mouse IL-4, -IFN-γ, -IL-10, IL-17 and propidium iodide (PI) (Biolegend); goat anti-digoxigenin, mouse anti-human CD3; mouse anti-human CD31 (AbD Serotec); rabbit anti-human Gal-1 (ATLAS Antibodies). Alexa Fluor® 488 donkey anti-mouse IgG, Alexa Fluor® 594 donkey anti-rabbit IgG, Alexa Fluor® 350 donkey anti-goat IgG (Invitrogen). PE-conjugated TRP-2 pentamer was purchased from Proimmune. Specific IgG1κ anti-ABCB5 mAb (3C2-1D12) was prepared as described(29, 30, 35, 36). TRIzol, DEPC-treated water, Platinum® PCR SuperMix High Fidelity, DTT, FBS, Zeocin, OPTI-MEM, Lipofectamine 2000, and protein-G agarose were from Invitrogen. 2-Acetamido-1,3,6-tri-O-acetyl-4-deoxy-4-fluoro-D-glucopyranose, 4-F-GlcNAc, was prepared as described(8, 9, 37). D-Glucosamine was purchased from Sigma Chemicals. TUNEL kit, including ApopTag TdT enzyme and reaction buffer, were purchased from Millipore.

Silencing of Gal-1 Expression.

The pLKO.1 vector encoding a short-hairpin RNA (shRNA) sequence against mouse Gal-1 (NM_008495) or encoding a non-silencing, scrambled shRNA control sequence was obtained from the RNAi Consortium (TRC) of the Broad Institute (MIT, Cambridge, MA) or from Addgene (Cambridge, MA), respectively. B16 melanoma cells were transduced with shRNA-expressing lentivirus and then selected in 1 g/ml puromycin dihydrochloride (Fisher). The target 21mer sequence of mouse Gal-1 recognized by the shRNA was: 5'-CCTACACTTCAATCCTCGCTT-3'. Gal-1 knockdown (Gal-1^{KD}) was >95% as confirmed by Western blotting and by real-time RT-PCR analysis with the following primer sequences: forward, 5'-TCTCAAACCTGGGGAATGTC-3', reverse, 5'-GCGAGGATTGAAGTGTAGGC-3'; and control ß-actin forward, 5'-CATCGTACTCCTGCTTGCTG-3' and reverse 5'-AGCGCAAGTACTCTGTGTGG-3'.

Production of B16 Melanoma Gal^{hi} Cells.

B16 melanoma cells were transfected with a previously reported plasmid encoding Gal-1 fused in frame to the Fc portion of human IgG (Gal-1hFc) (38).

Production of Gal-1hFc.

Gal-1hFc and non-ß-galactoside-binding mutant (dmGal-1hFc) were prepared as described (38).

Quantitative Real Time RT-PCR.

Quantitative real time RT-PCR was performed as previously described (38) using the primers: Gal-1 Forward: 5' TCTCAAACCTGGGGAATGTC 3', Reverse: 5' GCGAGGATTGAAGTGTAGGC 3' and ß-actin Forward: 5' CATCGTACTCCTGCTTGCTG 3', Reverse 5' AGCGCAAGTAC TCTGTGTGG. Samples were analyzed in triplicate and normalized to ß-actin expression.

Anchorage-Independent Soft Agar Assays. Primer sequesnces repeated

Assays were performed as previously described (39).

Gal-1 Ligand Expression Analysis.

Cells were analyzed for Gal-1 ligand expression using Gal-1hFc or dmGal-1hFc as previously described (38).

Western Blotting.

Gal-1 and ß-actin was immunoblotted as previously described (38).

***In vivo* T cell Activation.**

Dinitrofluorobenzene (DNFB)-skin draining lymph nodes (LN) were harvested 6d post-sensitization from mice treated with 100mg/kg 4-F-GlcNAc or glucosamine control on days 1, 3 and 5 post-sensitization , and analyzed by flow cytometry as previously described (38).

Treatment of Mice bearing B16 Melanoma or EL-4 lymphoma with 4-F-GlcNAc.

B16 melanoma wt, Gal^{hi} or Gal^{KD} cells were injected subcutaneously ($2x10^5$) into the right flank of 6-week old C57BL/6 wt, $CD43^{-/-}$, $Gal\text{-}1^{-/-}$ or $Rag2^{-/-}/Jak3^{-/-}$ mice (n=15 for each group, 5 mice per experiment). EL-4 lymphoma cells were injected subcutaneously ($5x10^5$) into the right flank of 6-week old C57BL/6 wt mice. Tumor development was monitored as described(18). Intraperitoneal injections of 4-F-GlcNAc or D-glucosamine (Sigma Chemicals) (each at 100mg/kg) were performed every other day starting on day 1 or 9 post-injection. Growth studies were terminated when tumors reached a volume greater than 1 cm^3.

Immunofluorescence.

Mouse tumor and LN tissues were stained with rabbit IgG anti-mouse CD3 (Abcam) and Gal-1hFc or dmGal-1hFc (20 g/ml) for 1h at room temperature, and subsequently incubated for 30 min with a cocktail of Cy-3 anti-rabbit IgG (Invitrogen) and rabbit anti-human IgG (Abcam), followed by a 30 min incubation with Cy-5 anti-rabbit IgG (Invitrogen) and counterstaining with DAPI. Alternatively, slides were stained with rabbit IgG anti-mouse CD3 and rat IgG anti-mouse Gal-1 (R&D Systems) for 1h at room temperature, and subsequently incubated for 30 min with a cocktail of Cy-5 anti-rabbit IgG and Cy-3 anti-rat IgG and counterstained with DAPI. Images were acquired using a Nikon eclipse Ti microscope and a Nikon FDX-35 digital camera.

Paraffin-embedded human melanoma specimens were stained for Gal-1 and ABCB5, CD31 or CD3 as previously reported (29). For TUNEL, Gal-1 and CD3 Immunofluorescence triple labeling; sections were incubated with TdT enzyme mixture, consisting of 77µl ApopTag reaction buffer and 33µl ApopTag TdT Enzyme, at 37°C for 1h. Sections were incubated with goat anti-digoxigenin, mouse anti-CD3, rabbit anti-Gal-1 overnight at 4°C, washed, and then incubated with Alexa Fluor® 350 donkey anti-goat IgG Alexa Fluor® 488 donkey anti-mouse IgG and Alexa Fluor® 594 donkey anti-rabbit IgG at room

temperature for 1h. Sections were analyzed with a BX51/BX52 microscope (Olympus). Images were captured using the CytoVision 3.6 software (Applied Imaging).

Pentamer Staining.

Tumor-draining LN were harvested on day 17 and minced, and single cell suspensions were blocked with anti-mouse CD16 (FcRγ) (1:100) for 10 minutes on ice, and immediately stained with 1 test PE-conjugated TRP-2 pentamers as described in the manufacturer's protocol. Cells were analyzed by flow cytometry by gating on $CD19^-/CD8^+$ cells.

Tumor cytotoxicity assays.

Memory ($CD62L^-$) $CD8^+$ T cells from tumor-draining LN were isolated 15 days post-inoculation by immunomagnetic bead sorting. Sorted $CD62L^-$ $CD8^+$ T cells were plated at incremental ratios with B16 or EL-4 tumor cells labeled with CFSE in 96-well round bottom plates. Naïve $CD62L^+$ $CD44^{lo}$ $CD4^+$ T cells were also obtained by immunomagnetic magnetic bead separation and used as negative tumor cytotoxicity control. After 6 hour incubation, cells were stained with 7-Amino-Actinomycin D (7-AAD) for 10 minutes and analyzed by flow cytometry.

Statistical Analyses. Statistical significance was ascertained between groups using a paired Student's *t*-test.

Online Supplemental Material. Please note that (7) Supplemental Figures and Legends are available online.

Results

Gal-1 creates an immune privilege site for melanoma-initiating cells.

ABCB5, a mediator of chemoresistance, has recently been described as a bona fide marker of human melanoma-initiating cells (29). $ABCB5^+$ melanoma cells possess greater tumorigenic activity and either differentiate into mature chemosensitive $ABCB5^-$ melanoma cells or maintain self-renewing potential. Furthermore, $ABCB5^+$ cells elicit an immunoregulatory signature on the tumor micro-environment, as they have been shown to decrease IL-2-dependent T cell proliferation, promote induction of $FoxP3^+$ Tregs and enhance IL-10 levels (30). Since these immunoregulatory features are similar to those created by Gal-1, we hypothesized that $ABCB5^+$ melanoma-initiating cells would synthesize higher amounts of Gal-1 than $ABCB5^-$ cells. To our surprise, immunofluorescence analyses on primary melanomas indicated that Gal-1 was overexpressed on distinct subsets of $ABCB5^-$ melanoma cells and not on $ABCB5^+$ cells (**Figure 1A and B**) or on cells positive for endothelial marker, CD31 (**Figure 1C**). However, Gal-1-overexpressing tumor cells frequently deposited Gal-1 in curvilinear arrays that encased $ABCB5^+$ cells (**Figure 1A and B**) and restricted $CD3^+$ T cells to the margin of these arrays (**Figure 1D and E**) or to separate zones (**Figure 1F**), suggesting that $Gal\text{-}1^+$ tumor cells could protect $ABCB5^+$ cells from immune clearance. Where $CD3^+$ T cells were in close proximity with $Gal\text{-}1^+$ cells, there was focal documentation of Gal-1 reactivity with T cell membranes (**Figure 1G and H**), which was associated with apoptotic activity (**Figure 1I**). To strengthen our finding that Gal-1 is differentially expressed on $ABCB5^+$ and $^-$ populations, we performed immunoblot and immunohistochemical analysis of Gal-1 on sorted $ABCB5^+$ or $^-$ human G3361 melanoma cells and found that $ABCB5^-$ cells were positive for Gal-1, whereas $ABCB5^+$ cells were negative (**Figure 1J and K**). These data help formulate the hypothesis that $Gal\text{-}1^+/ABCB5^-$ melanoma cells form an immunoprotective shield around $ABCB5^+$ cells to prevent effector T cells from entering cancer-initiating cell niches and that disrupting the Gal-1 – Gal-1 ligand axis can help circumvent tumor immune evasion.

Eliminating Gal-1 or Gal-1 ligand, CD43, inhibits effector cytokine expression and B16 melanoma growth.

To validate the role of Gal-1 in tumor immune evasion, we implemented the murine B16 melanoma cell model due to its ability to grow and metastasize in a Gal-1-dependent manner (14, 18, 40). As in human melanomas, we found that B16 melanomas contained $CD3^+$ T cells that were often marginalized and restricted to zones juxtaposed and reactive to Gal-1 expression (**Figure 1L**). To directly test Gal-1's role, we created B16 melanoma cell lines over-expressing Gal-1 (B16 Gal-1^{hi}) or silenced for Gal-1 expression (B16 Gal-1^{KD}). B16 Gal-1^{hi} cells expressed 25% more Gal-1 than wild type (wt) cells, and consisted of a Gal-1 molecule that is fused to a human immunoglobulin Fc domain to impart constitutively-active dimeric form (Gal-1hFc) (**Figure 2A and S1A**). Conversely, B16 Gal-1^{KD} cells, which were produced by RNA interference, exhibited 95% less Gal-1 (**Figure 2A and S1A**). Notably, all cell lines exhibited similar growth activity in anchorage-independent colony formation assays (**Figure S1B**).

Using these cell variants, we compared the tumor growth over 15 days and found that B16 Gal-1^{hi} tumors were larger than wt tumors (Student's paired *t*-test, $p<0.001$), whereas B16 Gal-1^{KD} tumors were smaller than wt tumors (Student's paired *t*-test; $P<0.01$) (**Figure 2B**). B16 Gal-1^{KD} tumors retained knockdown of Gal-1 expression, while B16 Gal-1^{hi} tumors maintained elevated expression of both native Gal-1 and transfected Gal-1hFc 15 days post inoculation (**Figure S1C**). Importantly, B16 Gal-1^{hi} or Gal-1^{KD} tumors grown in *Rag2*- and *Janus kinase* (*Jak)3*-doubly deficient mice, which lack in B, T and NK cells (34), were identical (**Figure 2C**), suggesting that Gal-1-associated differences in tumor growth were due to immune responsiveness.

We subsequently evaluated effector cytokines levels in tumor-draining lymph nodes (LN) in wt mice bearing B16 Gal-1^{hi} or Gal-1^{KD} tumors. As previously described(18), mice bearing Gal-1^{KD} tumors contained greater levels of IFN-γ^+ and IL-17^+ T cells, and lower levels of IL-10^+ leukocytes (**Figure 2D and E**) (Student's paired *t*-test, $p<0.001$). Interestingly, LN draining B16 Gal-1^{hi} tumors contained a 3-fold greater number of NKT cells when compared to those draining Gal-1^{KD} melanomas (**Figure S1D**). NKT cells have been found to suppress CTL responses in cancer by augmenting IL-13 levels and

enhancing activation of IL-4 STAT6 pathway (41), hence their presence may be contributing to Gal-1-mediated tumor immune evasion.

To determine the importance of leukocyte-expressed Gal-1 ligands in controlling B16 tumor growth, we performed tumor growth studies in mice lacking CD43, a putative Gal-1 ligand. CD43 is a constitutive leukocyte membrane protein that variably displays core 2 O-glycans depending on the activation status (42). The heavily-glycosylated form of CD43, which occurs after T cell activation, has been reported to be a major Gal-1 ligand mediating pro-apoptotic activity in effector T cells and inducing tolerogenic features in dendritic cells (16, 27). In an unrelated study, absence of CD43 in mice resulted in attenuated B16 melanoma growth and metastasis (28), but its role in Gal-1-mediated tumor immune evasion was not addressed. Here, we inoculated wt or $CD43^{-/-}$ mice with B16 wt or $Gal\text{-}1^{hi}$ cells and compared tumor growth rates. We found that in $CD43^{-/-}$ mice, B16 tumors independent of their Gal-1 expression grew at an identical rate and were significantly smaller than B16 $Gal\text{-}1^{hi}$ tumors grown in wt mice, suggesting that CD43 is an important component of Gal-1-mediated tumor immunity (Student's paired *t*-test, $p<0.001$) (**Figure 2F**). Based on the prominent role of tumor-derived Gal-1 in promoting tumor growth (**Figure 2B**), we also assessed whether host-derived Gal-1 might play a role by performing similar tumor growth experiments in Gal-1 deficient mice. Regardless of whether $Gal\text{-}1^{-/-}$ mice were inoculated with B16 wt or $Gal\text{-}1^{hi}$ cells, tumors in $Gal\text{-}1^{-/-}$ mice grew at a slower rate compared with $Gal\text{-}1^{hi}$ tumors grown in wt mice (Student's paired *t*-test, $p<0.001$) (**Figure 2G**). These data suggested that modifying host-derived Gal-1 or Gal-1 ligand expression may limit tumor growth.

4-F-GlcNAc inhibits the biosynthesis of Gal-1 ligands, sparing activated T cells from Gal-1-mediated death.

Gal-1 ligands are comprised of heavily-glycosylated membrane proteins displaying N- and O-glycans and, depending on antigen–experience and activation status, are found on both innate and adaptive immune cells. These glycans contain Gal-1-binding determinants consisting of N-acetyllactosamine Type1 (Galβ1,3GlcNAc) or Type 2 (Galβ1,4GlcNAc) disaccharides (22, 23). To demonstrate the expression and spatial location of Gal-1 ligands on immune cells in activated LN, we

painted abdominal skin with 0.5% DNFB (on day 0 and 1) and harvested LN draining DNFB-treated skin and non-draining LN and analyzed for T cell Gal-1 ligand expression by immunofluorescence with anti-CD3 and Gal-1hFc (38). As expected in **Figure 3A**, non-DNFB draining LN had limited numbers of Gal-1 ligand$^+$ T cells. However, LN-draining DNFB-treated skin exhibited intense Gal-1hFc staining on T cells residing in the paracortical and subcortical areas, with minimal reactivity in B cell zones (**Figure 3A**). Notably, Gal-1hFc staining co-localized with CD3$^+$ cells in a pattern suggestive of clonal expansion of activated T cells (**Figure 3A**). As a control, DNFB-draining LN did not stain with a non-binding mutant form of Gal-1hFc (dmGal-1hFc) (**Figure S2**). In addition, there were cells stained with Gal-1hFc that did not express CD3 and showed a macrophage/dendritic cell-like morphology, suggesting that Gal-1 ligands were also expressed on non-T cells in activated LN.

To determine whether lowering Gal-1 ligand expression increases the number of effector T cells and boosts anti-tumor immunity, we employed treatments with a fluorosugar inhibitor of N-acetyllactosamine biosynthesis, peracetylated 4-fluorinated glucosamine (4-F-GlcNAc). 4-F-GlcNAc has been shown to inhibit the formation of N-acetyllactosamines on T cells and Gal-1-binding determinants on ovarian and colon cancer cells (8, 9, 31-33, 43). Stability analysis of 4-F-GlcNAc in mouse plasma showed that the parent compound, fully acetylated 4-F-GlcNAc exhibited a half life of ~2.3h, indicating that O-acetylated side chains are rapidly metabolized to yield the active compound (**Figure S3A**). We first evaluated 4-F-GlcNAc-dependent abrogation of Gal-1 ligand synthesis on lymphocytes from LN draining DNFB-sensitized skin of mice treated with 100mg/kg 4-F-GlcNAc or glucosamine control. As previously shown (38), non-activated Th cells did not bind Gal-1hFc, whereas robust Gal-1hFc staining was evident on Th cells expressing the early activation marker, CD69 (**Figure 3B and C**). In contrast, Gal-1hFc binding on activated Th cells of 4-F-GlcNAc-treated mice was markedly reduced, while the number of CD69$^+$ cells remained unchanged (**Figure 3B**). In all assays, use of lactose-containing buffers confirmed ß-galactoside-dependent binding activity of Gal-1hFc. To assay whether inhibiting Gal-1 ligand formation with 4-F-GlcNAc also prevented Gal-1-mediated apoptosis, *ex vivo*-sorted naïve Th cells were activated with anti-CD3/anti-CD28 in the presence or absence of 4-F-GlcNAc for 48h and then exposed to 2.5 M Gal-1hFc with or without lactose control for

12h. FACS staining with PI and Annexin V revealed that 4-F-GlcNAc treatment significantly lowered the number of PI/Annexin V double positive cells compared untreated cells (Student's paired *t*-test, p<0.001) (**Figure 3D and E**). Inhibition of PI/Annexin V positivity with lactose confirmed the dependence of ß-galactoside-dependent Gal-1-binding for cell death induction.

4-F-GlcNAc decreases melanoma growth and Gal-1 ligand synthesis on effector T and NK cells.

To ascertain whether 4-F-GlcNAc-dependent lowering of Gal-1 ligands on activated T cells translates to enhanced anti-tumor immunity, wt mice (n=15/group) inoculated with B16 wt cells were treated with 100mg/kg 4-F-GlcNAc or glucosamine control every other day for 16 days. Compared with control glucosamine treatment, 4-F-GlcNAc significantly inhibited tumor growth (**Figure 4A**) (Student's paired *t*-test, p<0.001). Even on established tumors, 4-F-GlcNAc treatment from day 9 through day 16 also significantly attenuated tumor growth (Student's paired *t*-test, p<0.001) (**Figure 4A**). When 4-F-GlcNAc treatments were evaluated in CD43- or Gal-1-deficient mice bearing B16 tumors, tumor growth was almost completely prevented (Student's paired *t*-test, p<0.01) (**Figure 4B**). To analyze the presence of Gal-1 ligand$^+$ T cells in these tumors, we immunostained formalin-fixed paraffin-embedded tumors with Gal-1hFc and anti-CD3 mAb (**Figure 4C and S4**). These data showed that 4F-GlcNAc-treated mice had 5.4-fold more tumor-infiltrating CD3$^+$ cells than control-treated mice (**Figures 4C and S4**), and that 92.4% ± 4.3 of CD3$^+$ cells infiltrating tumors of control-treated mice expressed Gal-1 ligands (as well as some non-CD3$^+$ cells forming vascular-like structures) (**Figure 4C and S4**). However, in tumors from 4-F-GlcNAc-treated mice, we observed massive infiltrates of CD3$^+$ cells that express reduced levels of Gal-1 ligands (42.1% ± 11.7) (**Figures 4C and S4**). To validate modification of Gal-1 ligand expression on effector anti-tumor immunocytes from 4-F-GlcNAc-treated mice, tumor-draining LN were harvested and Gal-1 ligand expression was assayed on Th cells and CTLs and on NK cells. Results showed that Gal-1 ligand expression was significantly inhibited on all three subsets (Student's paired *t*-test, *p<0.01 or **p<0.001) (**Figure 4D and S3B**) and that CD43 was a major Gal-1 ligand on all three subsets (**Figure S3B**). To show that tumor cell-specific CTL death was spared in 4-F-GlcNAc-treated mice, we stained cells from tumor-draining LN with a pentamer recognizing B16-

melanoma epitope TRP-2 (180-188/H2Kb), TCR-specific CTLs(44). We found that TRP-2-specific $CD8^+$ T cells were elevated 2-fold compared with control glucosamine treatment and that TRP-2-specific T cell levels in 4-F-GlcNAc-treated $CD43^{-/-}$ mice were 3-fold greater compared with control treated wt mice (Student's paired *t*-test, $p<0.01$) (**Figure 5A and B**). Notably, in control treated Gal-$1^{-/-}$ mice bearing B16 tumors, a 3-fold higher level of TRP-2-specific CTLs was also evident compared with control treated wt mice, cementing Gal-1's role in regulating effector anti-tumor T cell levels. Additionally, we sorted memory ($CD62L^-$) CTLs from tumor draining LN, and co-cultured them *ex vivo* at incremental ratios of B16 tumor cells (**Figure 5C**). At 6h post-exposure, we found that CTLs from 4-F-GlcNAc-treated mice induced significantly more tumor cytotoxicity as determined by 7-AAD uptake than controls (Student's paired *t*-test, $p<0.05$) (**Figure 5C and S3C**). Notably, increased cytotoxicity paralleled the amount of CTLs present in the B16/T cell mixed culture, while no significant tumor cell death was observed in naïve Th cell co-cultures (**Figure 5C and S3C**). These data suggested that attenuated B16 tumor growth rates in 4-F-GlcNAc-treated, Gal-$1^{-/-}$ and/or $CD43^{-/-}$ mice may have been due to higher levels of effector anti-tumor CTLs.

To validate whether 4-F-GlcNAc-dependent Gal-1 ligand lowering on effector lymphocytes was responsible for anti-tumor responses, we performed experiments in $Rag2^{-/-}/Jak3^{-/-}$ mice lacking B, T and NK cells and found that B16 tumor growth rates were identical (**Figure S5**). These data suggest that altering Gal-1 ligand synthesis on effector anti-tumor immune cells with 4-F-GlcNAc was necessary for augmenting anti-tumor immune activity.

4-F-GlcNAc increases IFN-γ^+ T cell levels and lowers IL-10^+ T cell levels.

We and others have shown that Gal-1 not only promotes apoptosis on effector immune cells, but can also promote Th2 cell differentiation and IL-10 cytokine secretion (16, 17, 38, 45, 46). Therefore, we hypothesized that by abrogating Gal-1 ligand formation on effector T cells, we could prevent Gal-1-mediated Th2 skewing and IL-10 production and perhaps increase levels of IFN-γ, which has been described as a key determinant in T cell-directed anti-melanoma responses (18, 47). Accordingly, 15 days post-injection, we analyzed the cytokine profiles of Th and CTLs of B16 tumor-

draining LN in 4-F-GlcNAc- and control-treated mice. We found that, compared with glucosamine control treated mice, 4-F-GlcNAc-treated mice exhibited significantly higher levels of IFN-γ^+ Th and CTLs (Student's paired *t*-test, p<0.01) (**Figure 6A, B and F**). Similar elevations in IFN-γ were observed in CD43- and Gal-1-deficient mice treated with 4-F-GlcNAc, even though baseline levels of IFN-γ in control groups were higher than those in wt mice (**Figure 6A, B and F**). In contrast, IL-10^+ Th cells were significantly diminished in mice treated with 4-F-GlcNAc (Student's paired *t*-test, p<0.01) (**Figure 6C and F**). Of note, the number of IL-10^+ cells from control treated CD43- and Gal-1-deficient mice were markedly decreased compared with wt mice (**Figure 6C**), confirming the role of both molecules in Gal-1-mediated induction of IL-10 synthesis. Furthermore, we did not observe significant variation in IL-4 and IL-17 levels in wt mice after 4-F-GlcNAc treatment, though a significant in elevation in IL-17 expression was noted in CD43- or Gal-1-deficient mice treated with 4-F-GlcNAc (**Figure 6D, E and F**).

4-F-GlcNAc decreases EL-4 lymphoma growth and Gal-1 ligand expression on effector T and NK cells, by increasing IFN-γ and diminishing IL-10 levels.

To strengthen observations of 4-F-GlcNAc efficacy on effector anti-tumor immune cells and corresponding anti-tumor activity, we performed identical experiments in mice bearing a syngeneic EL-4 lymphoma that expresses Gal-1 (**Figure 7A**). As expected, there was a dramatic reduction in EL-4 tumor size in 4-F-GlcNAc-treated (wt and Gal-$1^{-/-}$) mice compared with those in control glucosamine treated mice (Student's paired *t*-test, p<0.001) (**Figure 7B and C**). We found that Th cells and CTLs, as well as NK cells from tumor draining LN showed diminished expression of Gal-1 ligands after 4-F-GlcNAc treatment (**Figure 7D**) and concomitant increased levels of IFN-γ^+ Th cells and CTLs when compared to the glucosamine-treated control (**Figure 7E and S7D**). Similar results on IFN-γ expression were also observed in Gal-$1^{-/-}$ mice (**Figure S6A and E**). We also found minor elevations in IL-17^+ T cells in 4-F-GlcNAc-treated wt and Gal-$1^{-/-}$ mice (**Figure S6C and E**). Conversely, IL-10^+ Th cells were significantly diminished in 4-F-GlcNAc-treated wt and in Gal-$1^{-/-}$ mice (Student's paired *t*-test, p<0.001) (**Figure 7E and S6B and D**). Accordingly, we observed enhanced tumor cytolytic activity in co-cultures of EL-4 tumor cells and CTLs cells from tumor-draining LN of wt or Gal-$1^{-/-}$ mice treated with

4-F-GlcNAc (**Figures S7A and B**). These data corroborated 4-F-GlcNAc inhibitory effects on B16 tumor growth and stimulatory effects on effector anti-tumor immunocyte levels.

Discussion

There is compelling evidence suggesting that Gal-1 helps establish immune privilege in cancer (18). Gal-1 has been shown to hamper the vitality of effector anti-tumor T cells and production of anti-tumor cytokine, IFN-γ, while inducing the expression of immunoregulators, IL-10 and regulatory T cells (17, 18, 47). To provide direct histological evidence illustrating Gal-1's role in tumor immunoprotective hypothesis, we performed immunofluorescence of Gal-1 and T cells in human melanomas. We found that Gal-1 is over-expressed on tumor cells that frequently deposit Gal-1 in a curvilinear pattern surrounding ABCB5$^+$ melanoma-initiating cells (29, 30). Furthermore, we found that Gal-1 is associated with T cells undergoing apoptosis at outer edge of the protective Gal-1$^+$ cellular boundary. We speculate that this immunoprotective "shield" helps prevent T cell infiltration into the core of these melanoma-initiating cell nests.

To analyze the dependence of Gal-1 ligands in Gal-1-mediated tumor immune evasion, we used a fluoro-glucosamine inhibitor of N-acetyllactosamine formation, 4-F-GlcNAc. This inhibitor, while the precise mechanism of anti-carbohydrate action is not fully understood, suppresses N-acetyllactosamine formation on glyco-metabolically active T cells and prevents consequent lectin-binding activity, including binding to Gal-1 (8, 9, 31-33, 43). We first established that Gal-1 ligand diminution on activated T cells via 4-F-GlcNAc treatment *in vivo* can alleviate Gal-1-mediated apoptotic activity in activated T cells. This observation indicated that effector anti-tumor T cells in a 4-F-GlcNAc-treated mouse could expand without restriction from a Gal-1 checkpoint, and perhaps provide more immunologic regulators to create effective anti-tumor immune activity. To this end, we evaluated 4-F-GlcNAc-mediated anti-tumor and immunomodulation efficacy in mice bearing syngeneic tumors, whose growth and progression is dependent on effector T cell suppression controlled by Gal-1 (18). We treated mice bearing tumor expressing variable levels of Gal-1 with N-acetyllactosamine-lowering doses of 4-F-GlcNAc or used mice deficient in candidate Gal-1 ligand, CD43, as controls. We observed marked reductions in tumor growth using both experimental approaches along with ablation of Gal-1 ligand expression on effector T cells and NK cells and resultant elevations in IFN-γ$^+$ Th cells and CTLs and melanoma-specific CTLs and reductions in IL-10$^+$ T cells. Furthermore, increased tumor

cytolytic activity was observed on tumor cells co-cultured with memory CTLs from 4-F-GlcNAc-treated tumor-bearing mice. Importantly, we found that established tumors were also sensitive to 4-F-GlcNAc treatment, suggesting that anti-tumor immunity can be stimulated even after effector T cell subset differentiation has been imprinted in tumor-draining LN. Since Gal-1 has been shown to stimulate tumor angiogenesis and related metastatic potential (14, 40, 48), inhibition of Gal-1 ligand synthesis on tumor endothelial cells could explain for suppressed tumor growth. However, 4-F-GlcNAc was ineffective at slowing tumor growth in immunodeficient mice, implying that 4-F-GlcNAc-dependent immune cell protection may be more influential on tumor growth than on Gal-1 ligand-dependent tumor angiogenesis. These results suggested that 1.) Gal-1-binding N-acetyllactosamines are targetable moieties on effector Th cells and CTLs and NK cells, 2.) CD43 is a major Gal-1 ligand transmitting Gal-1-mediated immunoregulation and 3.) 4-F-GlcNAc treatment can interfere with N-acetyllactosamine formation to prevent Gal-1-mediated apoptosis and raise the level of anti-tumor immune cells.

Since tumor endothelial cells have also been shown to express Gal-1, it is possible that host-derived endothelial cells infiltrating and feeding tumors in mice can also secrete sufficient concentrations of Gal-1 to facilitate tumor immune evasion (14, 48). To address whether host-derived Gal-1 contributes to Gal-1-mediated tumor immune evasion, we investigated tumor growth in mice deficient in Gal-1. We show that tumor growth was attenuated in Gal-1 deficient mice and, compared with wt mice, displayed higher levels of IFN-γ^+ Th cells and CTLs, including melanoma-specific CTLs, and lower levels of IL-10^+ Th cells. Of note, when 4-F-GlcNAc treatment was included in tumor bearing Gal-$1^{-/-}$ mice, the tumors were even smaller and effector T cell populations were higher, suggesting that, to effectively interfere with the Gal-1 – Gal-1 ligand axis, Gal-1 from the host and the tumor or all prospective Gal-1 ligands need to be targeted to achieve maximal anti-tumor immune efficacy.

Because N-acetyllactosamines are key moieties for sialyl Lewis X and platelet (P)-/ leukocyte (L)- and endothelial (E)-selectin ligand formation, 4-F-GlcNAc treatment can also interfere with the capacity of T cells to traffic to inflamed sites. Indeed, 4-F-GlcNAc can alleviate T cell recruitment to inflamed skin by interfering with E-selectin ligand synthesis (31-33, 43). In studies performed here, while we demonstrate that Gal-1 ligands are significantly lowered on effector T cells following 4-F-

GlcNAc treatment, this inhibitory effect did not interfere with the ability of these cells to traffic to tumors. Unlike inflammation in the skin, which requires E- and P-selectin-binding activity on inflammatory leukocytes (49-51), the tumor vasculature, particularly in melanomas, does not express E-selectin or P-selectin (52). Hence, 4-F-GlcNAc-treated tumor-infiltrating T cells can mobilize to melanomas independent of E- and P-selectin-dependent binding activity and elicit anti-tumor activity. In addition, we have found that 4-F-GlcNAc treatment does not greatly affect L-selectin ligand expression on high endothelial venules and alter the distribution of pattern of naïve lymphocytes to secondary lymphoid organs (32). Thus, endothelial cells do not appear to be particularly sensitive to glycometabolic modulation *in vivo*.

Interestingly, while N-acetyllactosamines can serve as binding-partners for other galectins, there appeared to be a marked therapeutic specificity of 4-F-GlcNAc for Gal-1 ligand abrogation. Indeed, if Gal-9 ligands were disrupted due to 4-F-GlcNAc treatment, there may have been an immune neutralizing response or antagonism of the anti-tumor immune boost conferred by interference of Gal-1 ligand synthesis. That is, since Gal-9 has been shown to enhance anti-tumor immunity via TIM-3 engagement (53), disrupting the Gal-9 – Gal-9 ligand axis could have paradoxically promoted tumor growth.

Using a sensitive and specific analytical method to measure 4-F-GlcNAc in plasma, we found that the parent, fully-acetylated 4-F-GlcNAc compound was quickly deacetylated, which was entirely consistent with a very high clearance of the parent drug from systemic circulation *in vivo*. As described for other acylated sugars (54), metabolism of parent compound is presumably the result of ubiquitous esterases. Collectively, these findings suggest that metabolites of fully-acetylated 4-F-GlcNAc are responsible for 4-F-GlcNAc's activity *in vivo*. Efforts have been initiated to identify the major bioactive metabolites in plasma.

In summary, data show that the spatial orientation of Gal-1 in human melanomas is illustrative of an immune "shield" that surrounds and protects putative melanoma-initiating cells from effector anti-tumor T cells, highlighting Gal-1's potentially critical role in the tumorigenicity and/or progression of melanomas in patients. Furthermore, targeting the Gal-1 ligand arm of the Gal-1 – Gal-1 ligand axis

can boost anti-tumor immunity and suppress tumor growth, representing a new potentially effective mode of cancer treatment.

Acknowledgements

F.C.L designed the research, performed the experiments, analyzed the data and wrote the paper. M.O. designed the research, performed the experiments, analyzed the data and wrote the paper. S.R.B. designed the research, performed the experiments and analyzed the data. D.H. performed the experiments and analyzed the data. X.H. performed the experiments and analyzed the data. Q.Z. performed the experiments and analyzed the data. T.S. performed the experiments and analyzed the data. M.H.F. provided regents, performed the experiments and analyzed the data. K.L.M. provided reagents. J.G.S. performed the experiments and analyzed the data. G.F.M. performed the experiments and analyzed the data. C.J.D. conceived the study, designed the research, analyzed the data, wrote the paper and supervised all experimentation. This work was supported by an NIH/NCI RO1 grant CA118124 to C. Dimitroff, an NIH/NCCAM RO1 grant AT004268 to C. Dimitroff, an NIH/NCI SPORE grant CA093683, an NIH/NIAMS Harvard Skin Disease Research Center grant AR042689, and NIH/NCI RO1 grants CA138231 and CA113796 to M. Frank.

References

1. Rabinovich GA, Ilarregui JM. Conveying glycan information into T-cell homeostatic programs: a challenging role for galectin-1 in inflammatory and tumor microenvironments. Immunological reviews 2009;230(1):144-59.
2. Rabinovich GA, Liu FT, Hirashima M, Anderson A. An emerging role for galectins in tuning the immune response: lessons from experimental models of inflammatory disease, autoimmunity and cancer. Scandinavian journal of immunology 2007;66(2-3):143-58.
3. Rabinovich GA, Toscano MA. Turning 'sweet' on immunity: galectin-glycan interactions in immune tolerance and inflammation. Nature reviews 2009;9(5):338-52.
4. Jung EJ, Moon HG, Cho BI*, et al.* Galectin-1 expression in cancer-associated stromal cells correlates tumor invasiveness and tumor progression in breast cancer. International journal of cancer 2007;120(11):2331-8.
5. Andre S, Kojima S, Yamazaki N*, et al.* Galectins-1 and -3 and their ligands in tumor biology. Non-uniform properties in cell-surface presentation and modulation of adhesion to matrix glycoproteins for various tumor cell lines, in biodistribution of free and liposome-bound galectins and in their expression by breast and colorectal carcinomas with/without metastatic propensity. Journal of cancer research and clinical oncology 1999;125(8-9):461-74.
6. Sanjuan X, Fernandez PL, Castells A*, et al.* Differential expression of galectin 3 and galectin 1 in colorectal cancer progression. Gastroenterology 1997;113(6):1906-15.
7. Tinari N, Kuwabara I, Huflejt ME, Shen PF, Iacobelli S, Liu FT. Glycoprotein 90K/MAC-2BP interacts with galectin-1 and mediates galectin-1-induced cell aggregation. International journal of cancer 2001;91(2):167-72.
8. Woynarowska B, Dimitroff CJ, Sharma M, Matta KL, Bernacki RJ. Inhibition of human HT-29 colon carcinoma cell adhesion by a 4-fluoro-glucosamine analogue. Glycoconjugate journal 1996;13(4):663-74.
9. Woynarowska B, Skrincosky DM, Haag A, Sharma M, Matta K, Bernacki RJ. Inhibition of lectin-mediated ovarian tumor cell adhesion by sugar analogs. The Journal of biological chemistry 1994;269(36):22797-803.
10. Clausse N, van den Brule F, Waltregny D, Garnier F, Castronovo V. Galectin-1 expression in prostate tumor-associated capillary endothelial cells is increased by prostate carcinoma cells and modulates heterotypic cell-cell adhesion. Angiogenesis 1999;3(4):317-25.
11. Glinsky VV, Huflejt ME, Glinsky GV, Deutscher SL, Quinn TP. Effects of Thomsen-Friedenreich antigen-specific peptide P-30 on beta-galactoside-mediated homotypic aggregation and adhesion to the endothelium of MDA-MB-435 human breast carcinoma cells. Cancer research 2000;60(10):2584-8.
12. van den Brule F, Califice S, Garnier F, Fernandez PL, Berchuck A, Castronovo V. Galectin-1 accumulation in the ovary carcinoma peritumoral stroma is induced by ovary carcinoma cells and affects both cancer cell proliferation and adhesion to laminin-1 and fibronectin. Laboratory investigation; a journal of technical methods and pathology 2003;83(3):377-86.
13. Ozeki Y, Matsui T, Yamamoto Y, Funahashi M, Hamako J, Titani K. Tissue fibronectin is an endogenous ligand for galectin-1. Glycobiology 1995;5(2):255-61.
14. Thijssen VL, Postel R, Brandwijk RJ*, et al.* Galectin-1 is essential in tumor angiogenesis and is a target for antiangiogenesis therapy. Proceedings of the National Academy of Sciences of the United States of America 2006;103(43):15975-80.
15. Thijssen VL, Barkan B, Shoji H*, et al.* Tumor cells secrete galectin-1 to enhance endothelial cell activity. Cancer research;70(15):6216-24.
16. Ilarregui JM, Croci DO, Bianco GA*, et al.* Tolerogenic signals delivered by dendritic cells to T cells through a galectin-1-driven immunoregulatory circuit involving interleukin 27 and interleukin 10. Nature immunology 2009;10(9):981-91.
17. Juszczynski P, Ouyang J, Monti S*, et al.* The AP1-dependent secretion of galectin-1 by Reed Sternberg cells fosters immune privilege in classical Hodgkin lymphoma. Proceedings of the National Academy of Sciences of the United States of America 2007;104(32):13134-9.

18. Rubinstein N, Alvarez M, Zwirner NW*, et al.* Targeted inhibition of galectin-1 gene expression in tumor cells results in heightened T cell-mediated rejection; A potential mechanism of tumor-immune privilege. Cancer cell 2004;5(3):241-51.
19. Kopcow HD, Rosetti F, Leung Y, Allan DS, Kutok JL, Strominger JL. T cell apoptosis at the maternal-fetal interface in early human pregnancy, involvement of galectin-1. Proceedings of the National Academy of Sciences of the United States of America 2008;105(47):18472-7.
20. Stannard KA, Collins PM, Ito K*, et al.* Galectin inhibitory disaccharides promote tumour immunity in a breast cancer model. Cancer letters.
21. Salatino M, Croci DO, Bianco GA, Ilarregui JM, Toscano MA, Rabinovich GA. Galectin-1 as a potential therapeutic target in autoimmune disorders and cancer. Expert opinion on biological therapy 2008;8(1):45-57.
22. Karmakar S, Stowell SR, Cummings RD, McEver RP. Galectin-1 signaling in leukocytes requires expression of complex-type N-glycans. Glycobiology 2008;18(10):770-8.
23. Allen HJ, Ahmed H, Matta KL. Binding of synthetic sulfated ligands by human splenic galectin 1, a beta-galactoside-binding lectin. Glycoconjugate journal 1998;15(7):691-5.
24. Perillo NL, Pace KE, Seilhamer JJ, Baum LG. Apoptosis of T cells mediated by galectin-1. Nature 1995;378(6558):736-9.
25. Toscano MA, Bianco GA, Ilarregui JM*, et al.* Differential glycosylation of TH1, TH2 and TH-17 effector cells selectively regulates susceptibility to cell death. Nature immunology 2007;8(8):825-34.
26. Vespa GN, Lewis LA, Kozak KR*, et al.* Galectin-1 specifically modulates TCR signals to enhance TCR apoptosis but inhibit IL-2 production and proliferation. J Immunol 1999;162(2):799-806.
27. Pace KE, Lee C, Stewart PL, Baum LG. Restricted receptor segregation into membrane microdomains occurs on human T cells during apoptosis induced by galectin-1. J Immunol 1999;163(7):3801-11.
28. Fuzii HT, Travassos LR. Transient resistance to B16F10 melanoma growth and metastasis in CD43-/- mice. Melanoma research 2002;12(1):9-16.
29. Schatton T, Murphy GF, Frank NY*, et al.* Identification of cells initiating human melanomas. Nature 2008;451(7176):345-9.
30. Schatton T, Schutte U, Frank NY*, et al.* Modulation of T-cell activation by malignant melanoma initiating cells. Cancer research;70(2):697-708.
31. Descheny L, Gainers ME, Walcheck B, Dimitroff CJ. Ameliorating skin-homing receptors on malignant T cells with a fluorosugar analog of N-acetylglucosamine: P-selectin ligand is a more sensitive target than E-selectin ligand. The Journal of investigative dermatology 2006;126(9):2065-73.
32. Dimitroff CJ, Kupper TS, Sackstein R. Prevention of leukocyte migration to inflamed skin with a novel fluorosugar modifier of cutaneous lymphocyte-associated antigen. The Journal of clinical investigation 2003;112(7):1008-18.
33. Gainers ME, Descheny L, Barthel SR, Liu L, Wurbel MA, Dimitroff CJ. Skin-homing receptors on effector leukocytes are differentially sensitive to glyco-metabolic antagonism in allergic contact dermatitis. J Immunol 2007;179(12):8509-18.
34. Barthel SR, Wiese GK, Cho J*, et al.* Alpha 1,3 fucosyltransferases are master regulators of prostate cancer cell trafficking. Proceedings of the National Academy of Sciences of the United States of America 2009;106(46):19491-6.
35. Frank NY, Pendse SS, Lapchak PH*, et al.* Regulation of progenitor cell fusion by ABCB5 P-glycoprotein, a novel human ATP-binding cassette transporter. The Journal of biological chemistry 2003;278(47):47156-65.
36. Frank NY, Schatton T, Frank MH. The therapeutic promise of the cancer stem cell concept. The Journal of clinical investigation;120(1):41-50.
37. Sharma M, Bernacki RJ, Paul B, Korytnyk W. Fluorinated carbohydrates as potential plasma membrane modifiers. Synthesis of 4- and 6-fluoro derivatives of 2-acetamido-2-deoxy-D-hexopyranoses. Carbohydrate research 1990;198(2):205-21.
38. Cedeno-Laurent F, Barthel SR, Opperman MJ, Lee DM, Clark RA, Dimitroff CJ. Development of a nascent galectin-1 chimeric molecule for studying the role of leukocyte galectin-1 ligands and immune disease modulation. J Immunol;185(8):4659-72.

39. Widlund HR, Horstmann MA, Price ER*, et al.* Beta-catenin-induced melanoma growth requires the downstream target Microphthalmia-associated transcription factor. The Journal of cell biology 2002;158(6):1079-87.
40. Thijssen VL, Barkan B, Shoji H*, et al.* Tumor Cells Secrete Galectin-1 to Enhance Endothelial Cell Activity. Cancer research 2010.
41. Terabe M, Matsui S, Noben-Trauth N*, et al.* NKT cell-mediated repression of tumor immunosurveillance by IL-13 and the IL-4R-STAT6 pathway. Nature immunology 2000;1(6):515-20.
42. Daniels MA, Hogquist KA, Jameson SC. Sweet 'n' sour: the impact of differential glycosylation on T cell responses. Nature immunology 2002;3(10):903-10.
43. Dimitroff CJ, Bernacki RJ, Sackstein R. Glycosylation-dependent inhibition of cutaneous lymphocyte-associated antigen expression: implications in modulating lymphocyte migration to skin. Blood 2003;101(2):602-10.
44. Wells JW, Cowled CJ, Farzaneh F, Noble A. Combined triggering of dendritic cell receptors results in synergistic activation and potent cytotoxic immunity. J Immunol 2008;181(5):3422-31.
45. van der Leij J, van den Berg A, Harms G*, et al.* Strongly enhanced IL-10 production using stable galectin-1 homodimers. Molecular immunology 2007;44(4):506-13.
46. Motran CC, Molinder KM, Liu SD, Poirier F, Miceli MC. Galectin-1 functions as a Th2 cytokine that selectively induces Th1 apoptosis and promotes Th2 function. European journal of immunology 2008;38(11):3015-27.
47. Kortylewski M, Komyod W, Kauffmann ME, Bosserhoff A, Heinrich PC, Behrmann I. Interferon-gamma-mediated growth regulation of melanoma cells: involvement of STAT1-dependent and STAT1-independent signals. The Journal of investigative dermatology 2004;122(2):414-22.
48. Thijssen VL, Hulsmans S, Griffioen AW. The galectin profile of the endothelium: altered expression and localization in activated and tumor endothelial cells. The American journal of pathology 2008;172(2):545-53.
49. Staite ND, Justen JM, Sly LM, Beaudet AL, Bullard DC. Inhibition of delayed-type contact hypersensitivity in mice deficient in both E-selectin and P-selectin. Blood 1996;88(8):2973-9.
50. Hirata T, Furie BC, Furie B. P-, E-, and L-selectin mediate migration of activated CD8+ T lymphocytes into inflamed skin. J Immunol 2002;169(8):4307-13.
51. Catalina MD, Estess P, Siegelman MH. Selective requirements for leukocyte adhesion molecules in models of acute and chronic cutaneous inflammation: participation of E- and P- but not L-selectin. Blood 1999;93(2):580-9.
52. Weishaupt C, Munoz KN, Buzney E, Kupper TS, Fuhlbrigge RC. T-cell distribution and adhesion receptor expression in metastatic melanoma. Clin Cancer Res 2007;13(9):2549-56.
53. Nagahara K, Arikawa T, Oomizu S*, et al.* Galectin-9 increases Tim-3+ dendritic cells and CD8+ T cells and enhances antitumor immunity via galectin-9-Tim-3 interactions. J Immunol 2008;181(11):7660-9.
54. Lavis LD. Ester bonds in prodrugs. ACS chemical biology 2008;3(4):203-6.

Figure Legends

Figure 1. Analysis of the spatial distribution of Gal-1 expression in melanomas. Primary human melanomas **(A-I)** (n=3) and murine B16 melanomas **(L)** (n=3) were immunostained for Gal-1 **(A-I and L,** red**)**, CD31 **(C,** green**)**, ABCB5 **(A and B,** green**)** and CD3 (**D-I and L,** green) and counterstained with DAPI **(A-H and L,** blue**)**. Arrows in **(A)** and **(B)** indicate that ABCB5^{+} tumors cells were encased in Gal-1 deposits and/or Gal-1-overexpressing tumor cells that frequently formed curvilinear arrays (bars in **(A)** =100μm and in **(B)** =50μm). In **(C)**, arrows indicate that Gal-1 was not uniformly co-localized on cells expressing vascular marker, CD31 (bar =200μm). Dashed lines in **(D)**, **(E)** and **(F)** demarcate spatial evidence of Gal-1 expression/deposits restricting CD3^{+} T cell infiltration (bars in **(D)** =100μm and in **(E)** and **(F)** =200μm). Arrows in **(G), (H)** and **(L)** indicate that Gal-1 was reactive to CD3^{+} T cell membranes (bars in **(G)** and **(H)** = 25μm and in **(L)** = 100μm). Arrow in **(I)** indicates that TUNEL^{+} cells (blue) were associated with Gal-1-reactive CD3^{+} T cells. In **(J)** and **(K)**, immunohistochemical and immunoblot analysis of Gal-1 was performed on sorted human ABCB5^{+} or $^{-}$ G3361 melanoma cells. (bars =100μm). Experiments were repeated 3-times.

Figure 2. Interfering with the Gal-1 – Gal-1 ligand axis alters B16 melanoma progression in immunocompetent mice. Gal-1 from B16 Gal-1^{hi} and B16 Gal-1^{KD} cells was quantified by Western blotting **(A)**. Tumor growth in mice inoculated with B16 melanoma (n=15) was assayed. Statistically significant differences compared with wt tumor, *p<0.01 and **p<0.001 **(B)**. Tumor growth (mean±S.D) was assayed in Rag2$^{-/-}$/Jak3$^{-/-}$ immunodeficient mice (n=15) inoculated with B16 Gal-1^{hi} or B16 Gal-1^{KD} cells **(C)**. Cells from tumor-draining LNs were analyzed for IFN-γ, IL-10 and IL-17 expression by flow cytometry. Representative plots and statistical analysis from 3 independent experiments are displayed in **(D)** and **(E)**, respectively. Statistically significant differences compared with B16 Gal1^{hi} tumors; *p<0.01, **p<0.001 **(E)**. CD43$^{-/-}$ mice **(F)** or Gal-1$^{-/-}$ mice **(G)** were injected subcutaneously with wt or B16 Gal-1^{hi} tumor cells, and tumor growth was assessed every other day. Statistically significant difference compared with wt tumor cells grown in CD43$^{-/-}$ mice (**p<0.001) or in Gal-1$^{-/-}$ mice (***p<0.0001). Data represent mean ± SD of 3 independent experiments.

Figure 3. **Gal-1 ligands on activated T cells and Gal-1-mediated apoptosis are inhibited by 4-F-GlcNAc treatment.** **(A)** Immunofluorescence of CD3 (red) and Gal-1 ligands (green) was performed on LNs draining DNFB-sensitized skin. Representative microphotographs taken at 4X (upper and middle panels) and 10x (lower panel) are shown (Inset = 40x) (bars =100 m). **(B)** DNFB-abdominal skin sensitization as in **(A)** was performed in mice treated with 100mg/kg 4-F-GlcNAc or glucosamine control. Cells from DNFB-draining LNs were stained with anti-CD4, anti-CD69 and Gal-1hFc and analyzed by flow cytometry. **(C)** Naïve Th cells were activated *ex vivo* for 48h in the presence or absence 15μM 4-F-GlcNAc. Gal-1hFc staining in the presence or absence of lactose was then performed and cells analyzed by flow cytometry. **(D)** Activated T cells as prepared **(C)** were incubated with 2.5 M Gal-1hFc for 24h, and cell death was evaluated by Annexin V staining and PI uptake. **(E)** Graphical representation of data from 3 different experiments is shown as mean± SD Annexin V^+ staining/PI^+ uptake. Statistically significance difference compared with untreated cells, **p<0.001 and ***p<0.0001. To control for Gal-1hFc-binding, 50mM lactose was added to culture medium or buffers.

Figure 4. **4-F-GlcNAc diminishes Gal-1 ligands on T and NK cells and limits the growth of nascent and established B16 melanomas.** **(A)** Tumor growth was assayed in mice inoculated with B16 melanoma cells and treated every other day with 100mg/kg 4-F-GlcNAc or glucosamine control starting from day 1 or from day 9 (n=15/group). Statistically significant difference compared with no treatment, **p<0.001. Data represent the mean ± SD of 3 independent experiments. **(B)** Photographs of 3 representative tumors harvested on day 17 from wt, $CD43^{-/-}$ or Gal-$1^{-/-}$ mice treated or untreated with 4-F-GlcNAc (Left Panel). N.D. - tumors were not detected. Tumor size was calculated (mean ± SD) on day 17 from wt, $CD43^{-/-}$ or Gal-$1^{-/-}$ mice treated or untreated with 4-F-GlcNAc (n=15/group) (Right Panel). Statistically significant difference compared with no treatment, *p<0.01 and **p<0.001. **(C)** Immunofluorescence of Gal-1 ligands (green) and CD3 (red) and counterstaining with DAPI (blue) was performed on B16 melanomas from control- or 4-F-GlcNAc-treated mice. Representative microphotographs from 4 experiments are shown (bars =200 m). **(D)** On day 17, cells from tumor-draining LN of 4-F-GlcNAc or control-treated mice were stained with anti-CD4, anti-CD8, anti-NK1.1 and Gal-1hFc (with or without lactose) and analyzed by flow cytometry.

Figure 5. 4-F-GlcNAc enhances specific anti-B16 melanoma responses. (A) Wt, CD43$^{-/-}$ or Gal-1$^{-/-}$ mice inoculated with B16 melanoma cells (n=15/group) were treated every other day with 100mg/kg 4-F-GlcNAc or glucosamine control starting on day 1. CD8^{+}/CD19^{-} gated cells from tumor-draining LNs blocked with anti-CD16 mAb were analyzed by flow cytometry for TRP-2 pentamer binding. **(B)** Data are represented graphically from 3 different experiments. Bars represent mean ± SD TRP-2 binding. Statistically significant difference compared with control untreated group, *p<0.01. **(C)** Memory CTLs from 4-F-GlcNAc-treated or control-treated mice bearing B16 melanomas were co-cultured with CFSE-labeled B16 melanoma cells. After 6h, cultured cells were stained with 7-AAD, and cell viability of CFSE^{+} cells was analyzed by flow cytometry.

Figure 6. 4-F-GlcNAc elevates IFN-γ^{+} and IL-17^{+} T cell levels and decreases IL-10^{+} T cells. Wt, CD43$^{-/-}$ or Gal-1$^{-/-}$ mice inoculated with B16 melanoma cells (n=15/group) were treated every other day with 100mg/kg 4-F-GlcNAc or glucosamine control starting on day 1. CD4^{+} and CD8^{+} T cells from tumor-draining LN were analyzed for IFN-γ, IL-4, IL-10 and IL-17 expression by flow cytometry. Representative dot plots for CD4/IFN-γ **(A)**, CD8/IFN-γ **(B)**, CD4/IL-10 **(C)**, CD4/IL-4 **(D)** and CD4/IL-17 **(E)** are shown. **(F)** Graphical representation of data from 3 different experiments. Bars represent mean ± SD of % Double Positive Cells. Statistically significant difference compared with control untreated group, *p<0.01.

Figure 7. 4-F-GlcNAc diminishes Gal-1 ligands on T and NK cells and limits EL-4 lymphoma growth. (A) Expression of Gal-1 and loading control, ß-actin, on B16 and EL-4 tumors was compared by Western blot analysis. **(B)** Tumor growth was assayed in mice inoculated with EL-4 tumor cells and treated every other day with 100mg/kg 4-F-GlcNAc or glucosamine control for 15 days (n=5/group). Statistically significant difference compared with control treatment in wt mice, **p<0.001. Data represent mean ± SD of 3 independent experiments. **(C)** Photographs of 3 representative tumors from wt or Gal-1$^{-/-}$ mice treated or untreated with 4-F-GlcNAc (Left Panel). Tumor size (mean ± SD) on day 15 from wt or Gal-1$^{-/-}$ mice treated or untreated with 4-F-GlcNAc (n=6/group) is graphically represented (Right Panel). Statistically significant difference compared with control treatment, **p<0.001. **(D)** Cells from tumor draining LNs from wt or Gal-1$^{-/-}$ mice treated or untreated with 4-F-GlcNAc were stained with

anti-CD4, anti-CD8, anti-NK1.1 and Gal-1hFc (+/- lactose) and analyzed by flow cytometry. **(E)** Cells from tumor-draining LN cells were analyzed for IFN-γ, IL-4 and IL-10 expression by flow cytometry. Representative dot plots are shown.

Figure 1

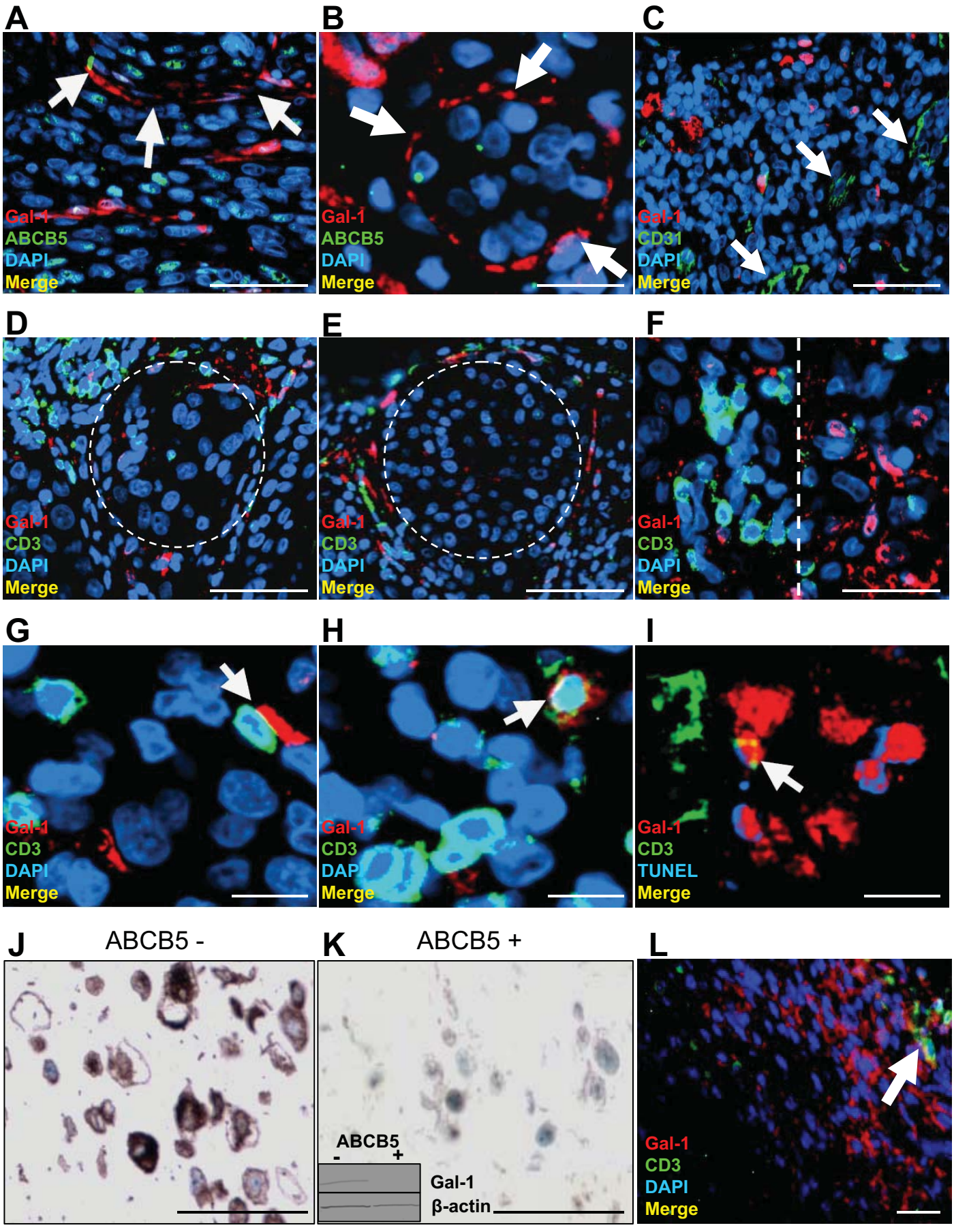
A
Gal-1
ABCB5
DAPI
Merge
B
Gal-1
ABCB5
DAPI
Merge
C
Gal-1
CD31
DAPI
Merge
D
Gal-1
CD3
DAPI
Merge
E
Gal-1
CD3
DAPI
Merge
F
Gal-1
CD3
DAPI
Merge
G
Gal-1
CD3
DAPI
Merge
H
Gal-1
CD3
DAP
Merge
I
Gal-1
CD3
TUNEL
Merge
J
ABCB5 -
K
ABCB5 +
ABCB5
-
+
Gal-1
β-actin
L
Gal-1
CD3
DAPI
Merge

Figure 2

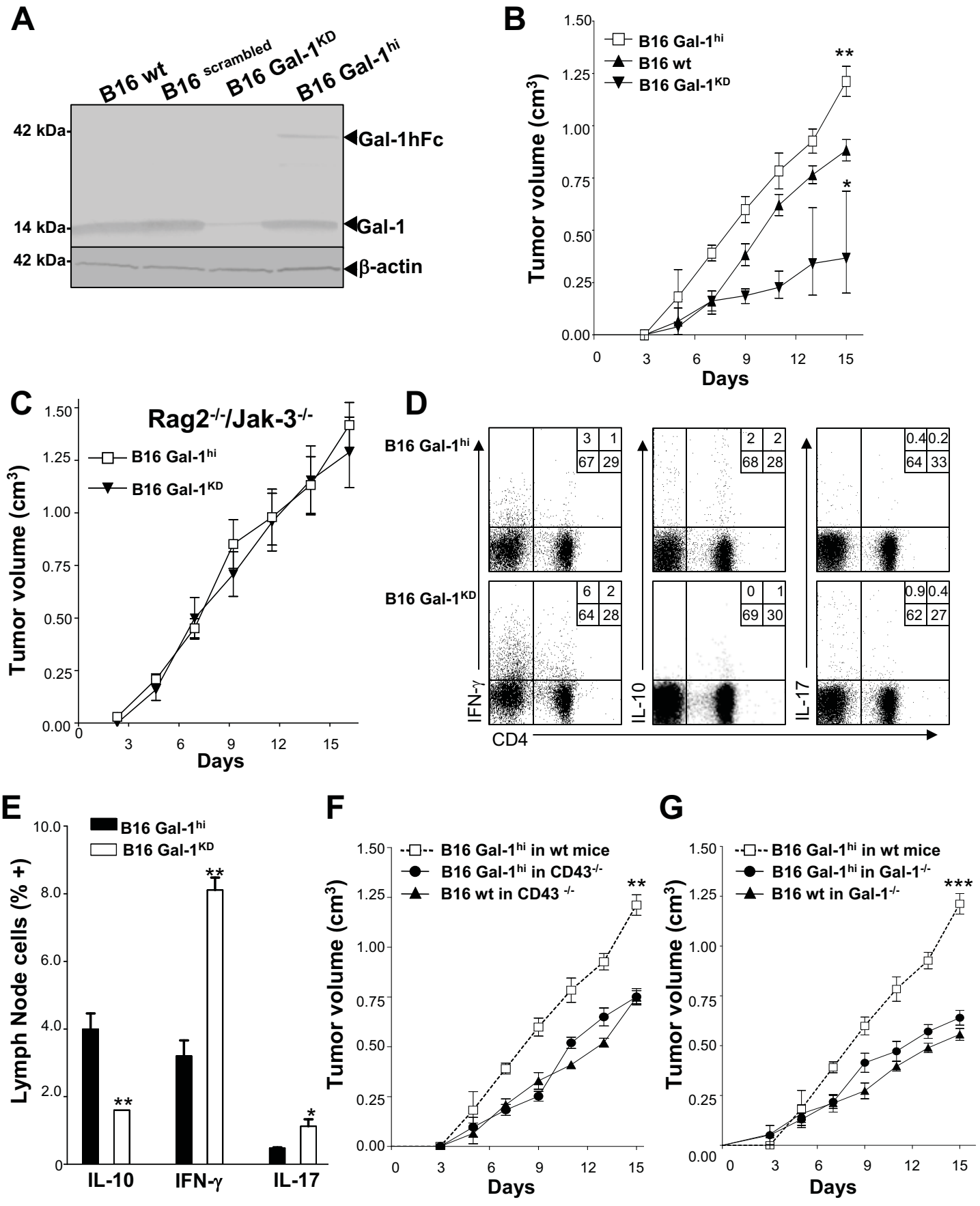
A
B16 wt
B16 scrambled
B16 Gal-1KD
B16 Gal-1hi
42 kDa
Gal-1hFc
14 kDa
Gal-1
42 kDa
β-actin
B
B16 Gal-1hi
B16 wt
B16 Gal-1KD
Tumor volume (cm3)
Days
C
Rag2-/-/Jak-3-/-
B16 Gal-1hi
B16 Gal-1KD
Tumor volume (cm3)
Days
D
B16 Gal-1hi
B16 Gal-1KD
IFN-γ
IL-10
IL-17
CD4
E
B16 Gal-1hi
B16 Gal-1KD
Lymph Node cells (% +)
IL-10
IFN-γ
IL-17
F
B16 Gal-1hi in wt mice
B16 Gal-1hi in CD43-/-
B16 wt in CD43 -/-
Tumor volume (cm3)
Days
G
B16 Gal-1hi in wt mice
B16 Gal-1hi in Gal-1-/-
B16 wt in Gal-1-/-
Tumor volume (cm3)
Days

Figure 3

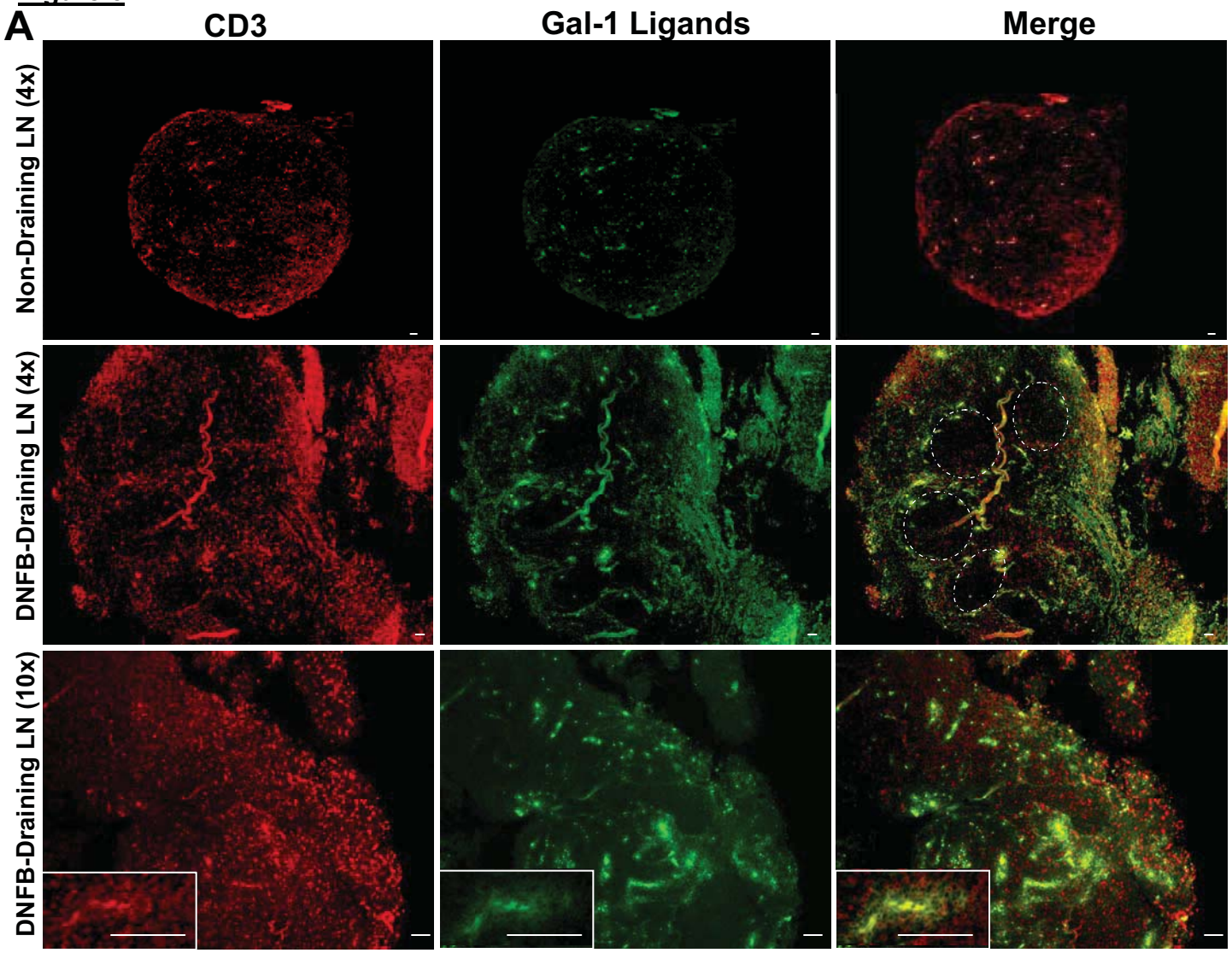
A
CD3
Gal-1 Ligands
Merge
Non-Draining LN (4x)
DNFB-Draining LN (4x)
DNFB-Draining LN (10x)

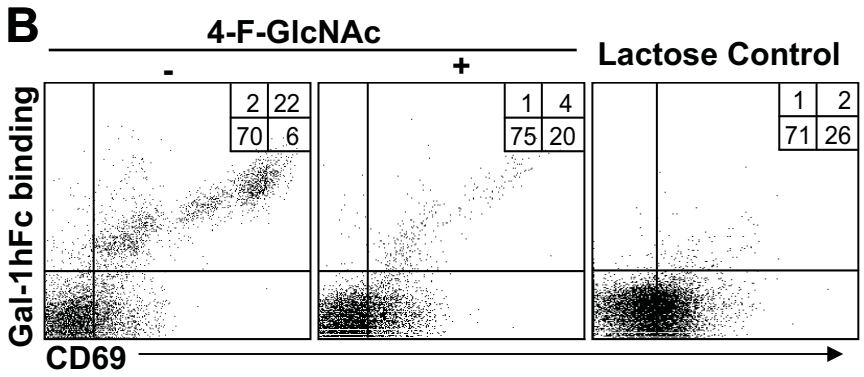
B
4-F-GlcNAc
Lactose Control
-
+
2 22 70 6
1 4 75 20
1 2 71 26
Gal-1hFc binding
CD69

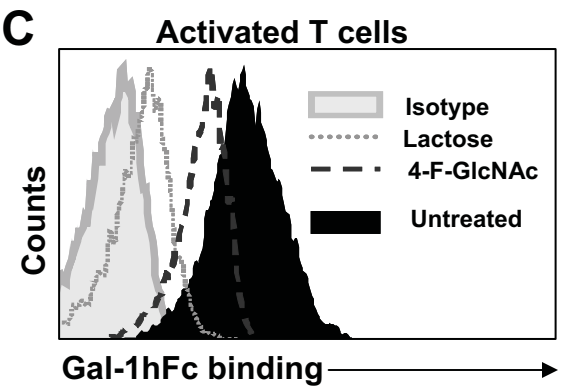
C
Activated T cells
Isotype
Lactose
4-F-GlcNAc
Untreated
Counts
Gal-1hFc binding

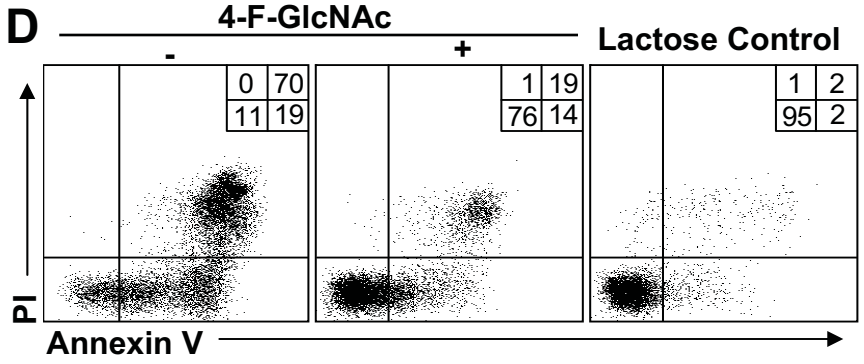
D
4-F-GlcNAc
Lactose Control
-
+
0 70 11 19
1 19 76 14
1 2 95 2
PI
Annexin V

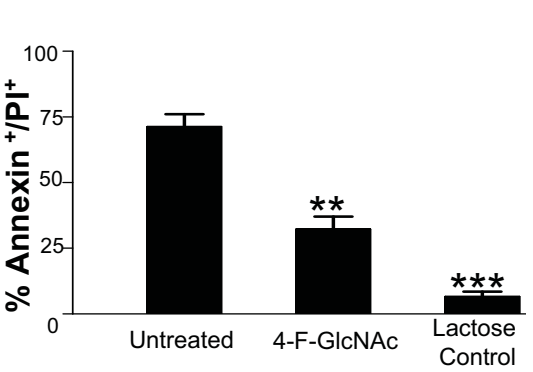
E
% Annexin +/PI+
100
75
50
25
0
**
***
Untreated
4-F-GlcNAc
Lactose Control

Figure 4

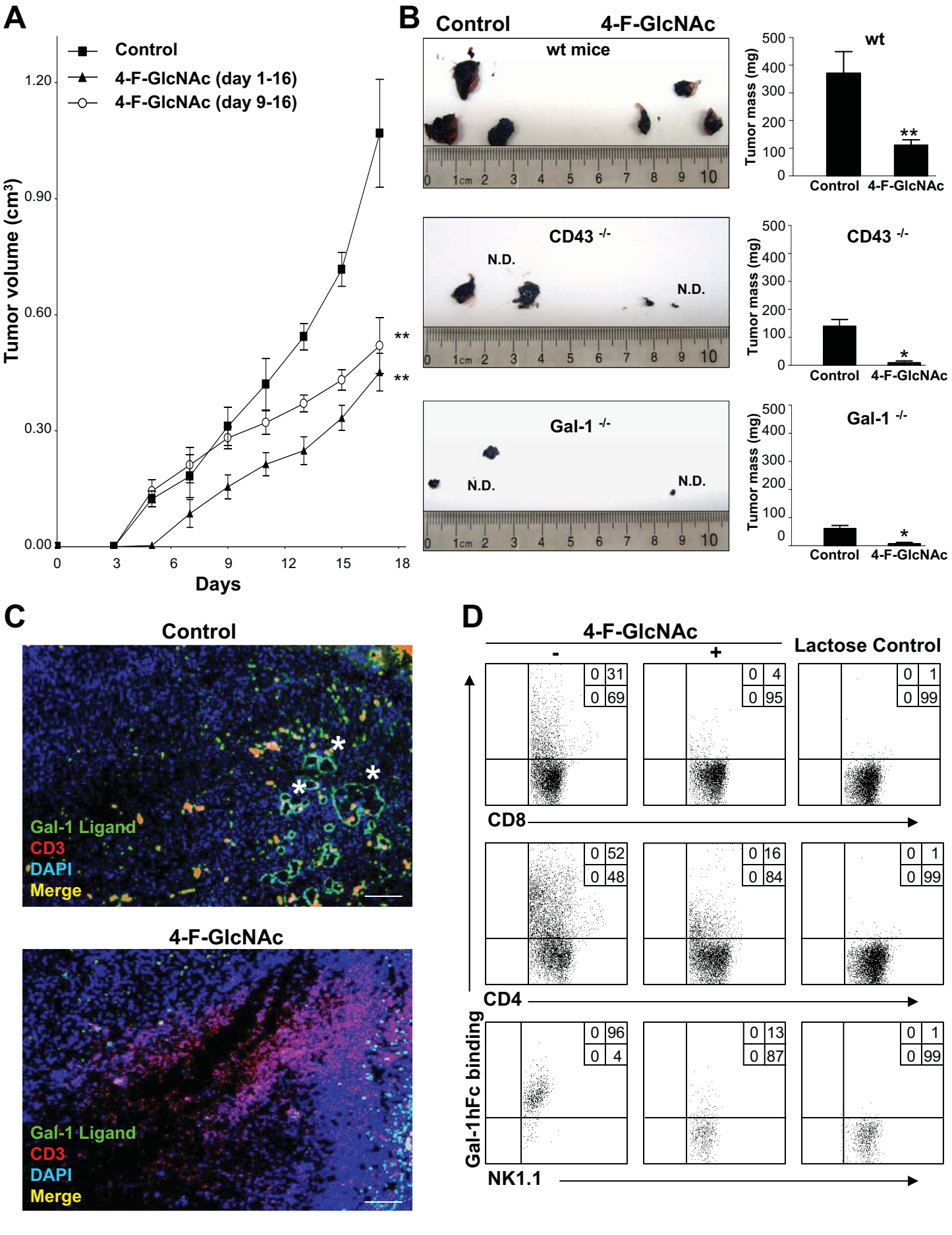
A
Control
4-F-GlcNAc (day 1-16)
4-F-GlcNAc (day 9-16)
Tumor volume (cm3)
1.20
0.90
0.60
0.30
0.00
0
3
6
9
12
15
18
Days
**
**
B
Control
4-F-GlcNAc
wt mice
CD43 -/-
N.D.
N.D.
Gal-1 -/-
N.D.
N.D.
1cm 2 3 4 5 6 7 8 9 10
Tumor mass (mg)
500
400
300
200
100
0
wt
**
Control
4-F-GlcNAc
CD43 -/-
*
Gal-1 -/-
*
C
Control
Gal-1 Ligand
CD3
DAPI
Merge
4-F-GlcNAc
Gal-1 Ligand
CD3
DAPI
Merge
D
4-F-GlcNAc
-
+
Lactose Control
0 31
0 69
0 4
0 95
0 1
0 99
CD8
0 52
0 48
0 16
0 84
0 1
0 99
CD4
0 96
0 4
0 13
0 87
0 1
0 99
Gal-1hFc binding
NK1.1

Figure 5

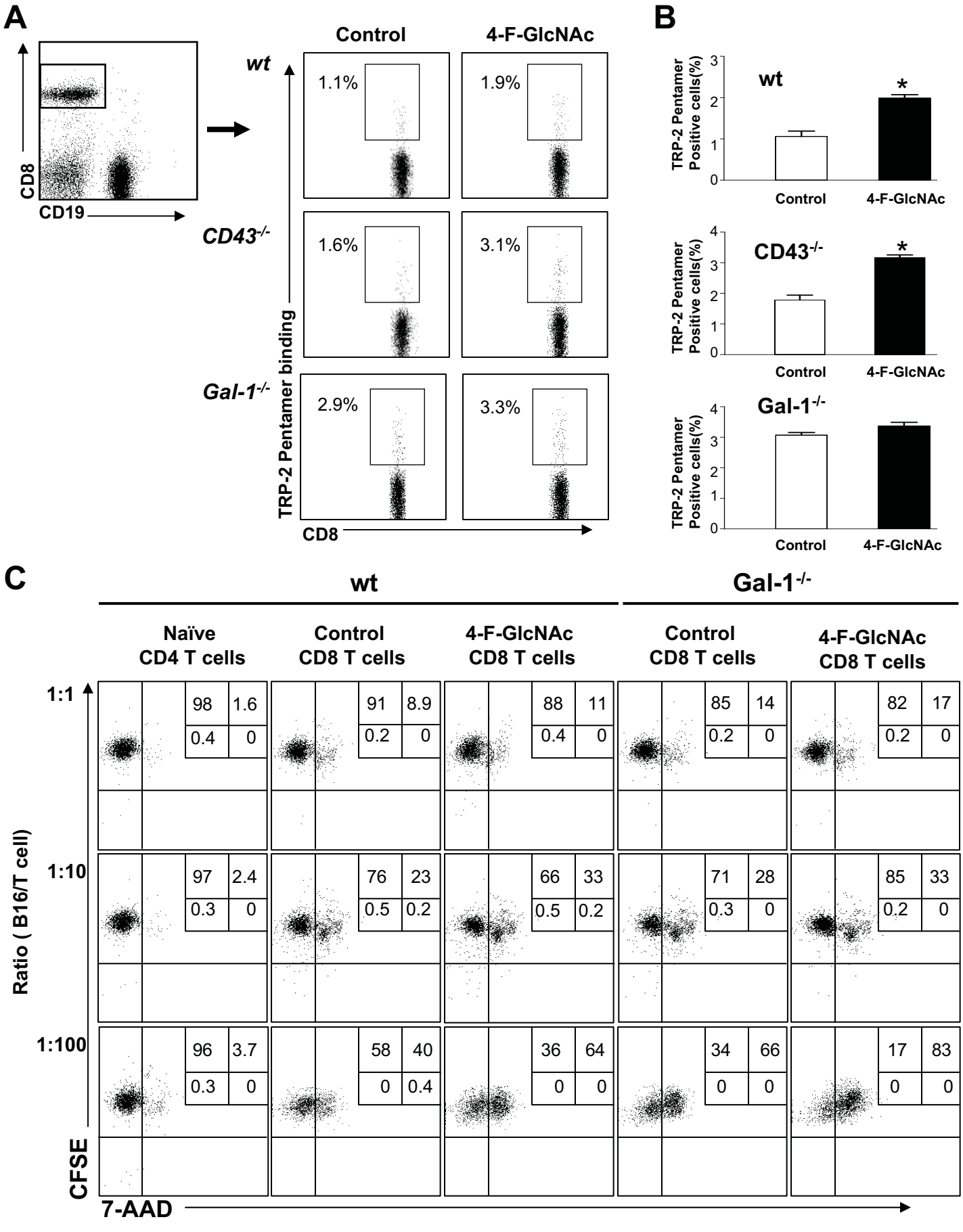
A
Control
4-F-GlcNAc
wt
CD43-/-
Gal-1-/-
1.1%
1.9%
1.6%
3.1%
2.9%
3.3%
CD8
CD19
TRP-2 Pentamer binding
CD8
B
wt
CD43-/-
Gal-1-/-
TRP-2 Pentamer Positive cells(%)
Control
4-F-GlcNAc
C
wt
Gal-1-/-
Naïve CD4 T cells
Control CD8 T cells
4-F-GlcNAc CD8 T cells
Control CD8 T cells
4-F-GlcNAc CD8 T cells
1:1
1:10
1:100
Ratio (B16/T cell)
CFSE
7-AAD
98 1.6 0.4 0
91 8.9 0.2 0
88 11 0.4 0
85 14 0.2 0
82 17 0.2 0
97 2.4 0.3 0
76 23 0.5 0.2
66 33 0.5 0.2
71 28 0.3 0
85 33 0.2 0
96 3.7 0.3 0
58 40 0 0.4
36 64 0 0
34 66 0 0
17 83 0 0

Figure 6

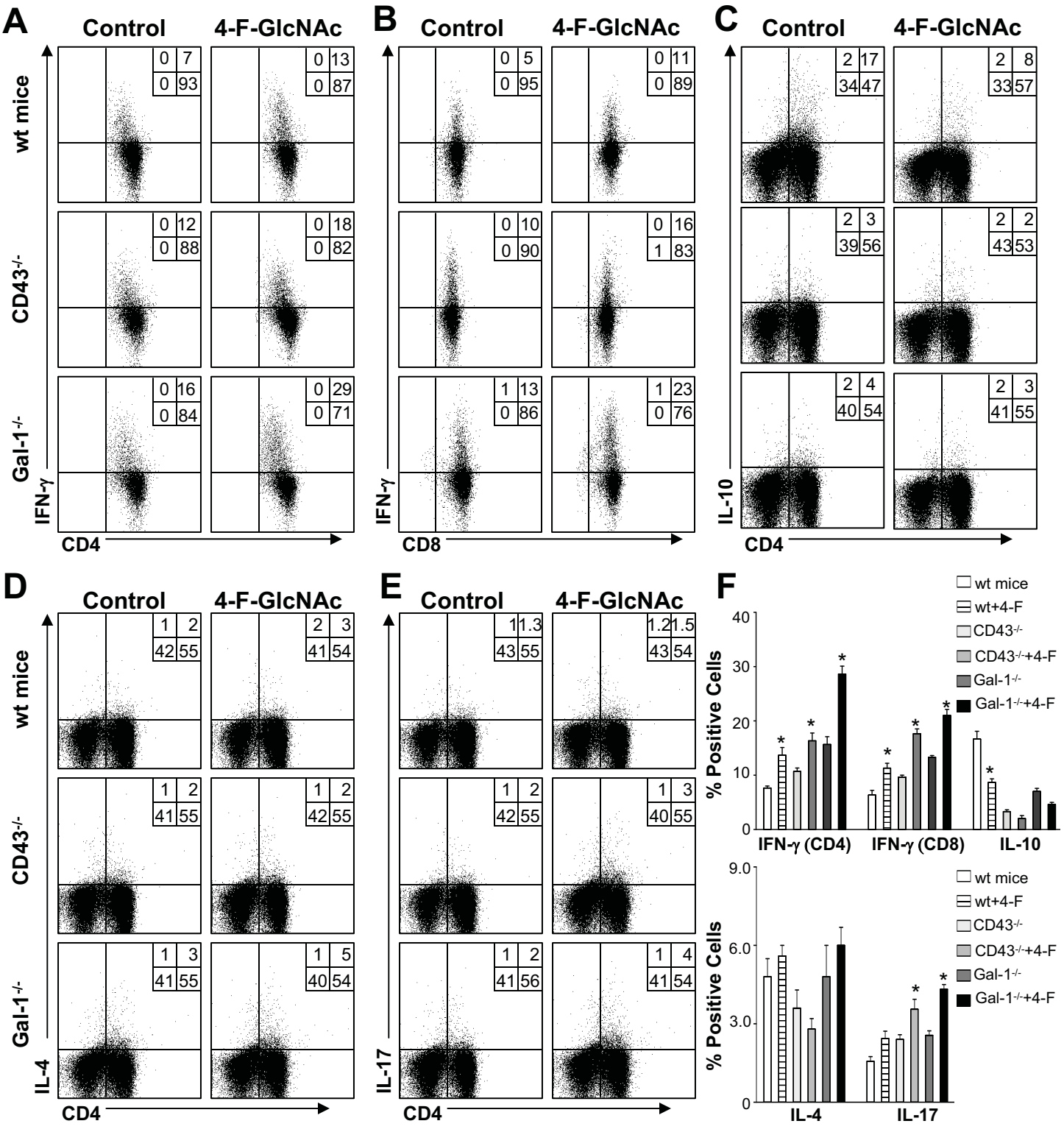
A
Control
4-F-GlcNAc
wt mice
CD43-/-
Gal-1-/-
IFN-γ
CD4
0 7
0 93
0 13
0 87
0 12
0 88
0 18
0 82
0 16
0 84
0 29
0 71
B
Control
4-F-GlcNAc
IFN-γ
CD8
0 5
0 95
0 11
0 89
0 10
0 90
0 16
1 83
1 13
0 86
1 23
0 76
C
Control
4-F-GlcNAc
IL-10
CD4
2 17
34 47
2 8
33 57
2 3
39 56
2 2
43 53
2 4
40 54
2 3
41 55
D
Control
4-F-GlcNAc
wt mice
CD43-/-
Gal-1-/-
IL-4
CD4
1 2
42 55
2 3
41 54
1 2
41 55
1 2
42 55
1 3
41 55
1 5
40 54
E
Control
4-F-GlcNAc
IL-17
CD4
1 1.3
43 55
1.2 1.5
43 54
1 2
42 55
1 3
40 55
1 2
41 56
1 4
41 54
F
wt mice
wt+4-F
CD43-/-
CD43-/-+4-F
Gal-1-/-
Gal-1-/-+4-F
% Positive Cells
0
10
20
30
40
IFN-γ (CD4)
IFN-γ (CD8)
IL-10
% Positive Cells
0
3.0
6.0
9.0
IL-4
IL-17

Figure 7

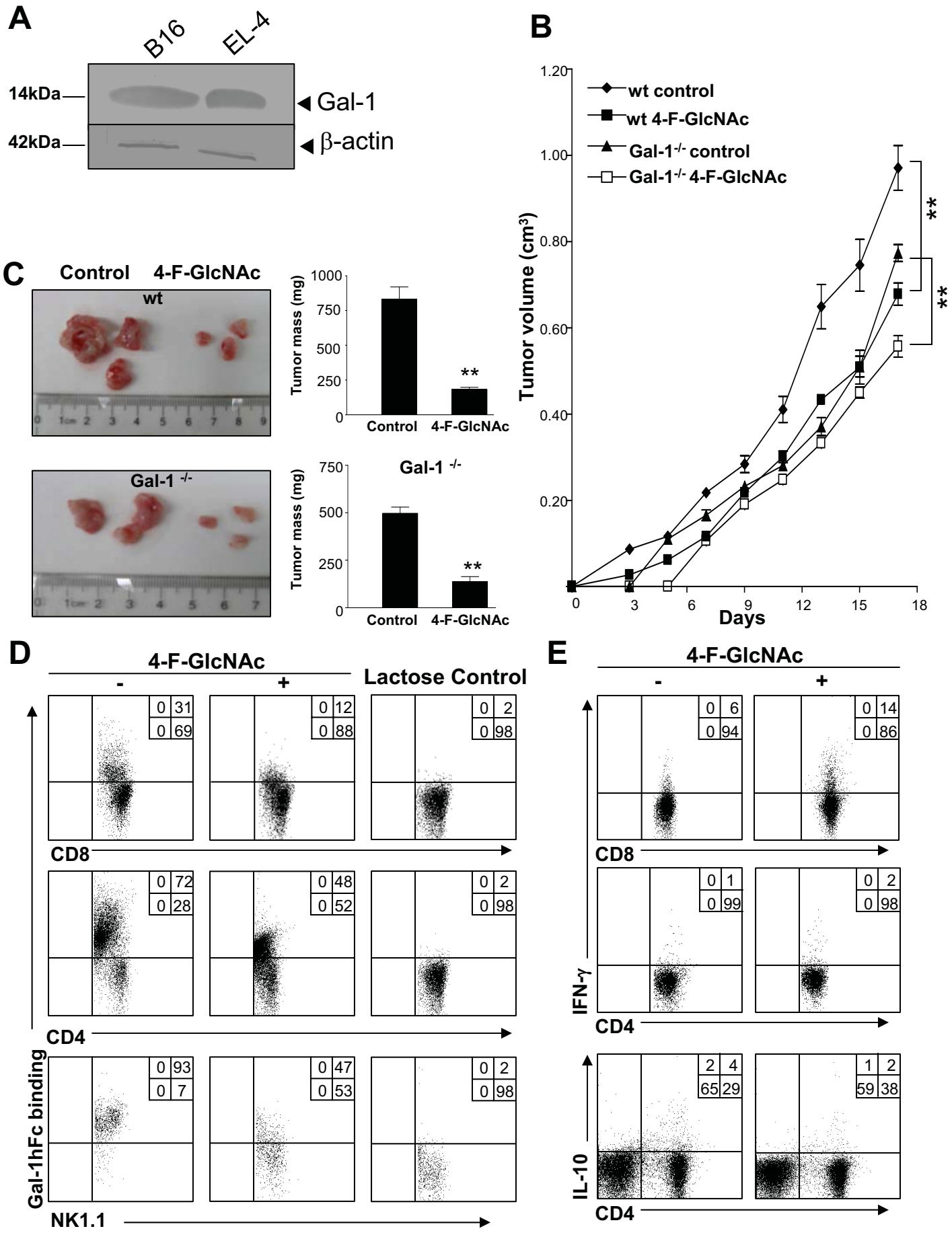
A
B16
EL-4
14kDa
42kDa
Gal-1
β-actin
B
wt control
wt 4-F-GlcNAc
Gal-1-/- control
Gal-1-/- 4-F-GlcNAc
Tumor volume (cm3)
Days
**
**
C
Control
4-F-GlcNAc
wt
Gal-1 -/-
Tumor mass (mg)
Control
4-F-GlcNAc
**
D
4-F-GlcNAc
Lactose Control
CD8
CD4
Gal-1hFc binding
NK1.1
E
IFN-γ
IL-10